Spatio-Temporal Dynamics in a Ring of Coupled Pendula: Analogy with Bubbles

V.J. Sánchez-Morcillo, N. Jiménez, J. Chaline, A. Bouakaz, and S. Dos Santos

Abstract Many systems in nature, like drops, bubbles or some macromolecules present circular or spherical symmetry. Under the influence of some external force, such objects often develop surface patterns whose properties are greatly influenced by the underlying geometry. However, differently from the planar case, patterns in curved geometries have been much less explored. Despite the complexity of the particular physical problems, the basic dynamical features are often captured by simple models of coupled oscillators. Here we present a theoretical and experimental study of the spatial instabilities of circular ring of coupled pendula parametrically driven by a vertical harmonic force. Normal oscillation modes (breathing, dipole, quadrupole) and localized patterns of different types (breathers and kinks) are predicted and observed. The analogy between the considered discrete mechanical system and a gas bubble cavitating under the action of an acoustic field is established. On the basis of this analogy, the oscillation patterns and localized modes observed experimentally in acoustically driven bubbles are interpreted and discussed.

V.J. Sánchez-Morcillo (✉) · N. Jiménez
Instituto de Investigación para la Gestión, Integrada de las Zonas Costeras,
Universitat Politécnica de Valencia, c/ Paranimf no. 1, 46730 Grao de Gandia, Spain
e-mail: victorsm@upv.es

J. Chaline · A. Bouakaz
Unité Mixte de Recherche Inserm U930 "Imagerie et Cerveau, Université François-Rabelais
PRES Centre Val de Loire Université, 10 boulevard Tonnellé, 37032 Tours Cedex, France

S. Dos Santos
ENI Val de Loire, 3 Rue de la Chocolaterie BP 3410, F-41034 Blois cedex, France

Unité Mixte de Recherche Inserm U930 "Imagerie et Cerveau, Université François-Rabelais
PRES Centre Val de Loire Université, 10 boulevard Tonnellé, 37032 Tours Cedex, France

R. Carretero-González et al. (eds.), *Localized Excitations in Nonlinear Complex Systems*,
Nonlinear Systems and Complexity 7, DOI 10.1007/978-3-319-02057-0_13,

© Springer International Publishing Switzerland 2014

1 Introduction

The spatio-temporal dynamics of a gas bubble in a fluid under the action of an external oscillating pressure field has been the subject of intense investigations during the last decades [1]. An acoustically forced bubble experiences different instabilities as the driving parameters (mainly the amplitude and the frequency of the external field) are changed. One of such instabilities leads to the formation of surface patterns, similar to the Faraday patterns observed in the free surface of vertically vibrated fluids, by means of parametric excitation of subharmonic modes [2,3]. Nonlinear patterns on the bubble surface have been however much less explored. Only recently, the existence of localized soliton-type surface waves has been theoretically considered [11]; their existence has been evidenced by different experimental observations. An interesting extension is the bubble with an artificial coating, so called ultrasound contrast agent (UCA), with current applications in medical imaging and different therapies. Besides free gas bubbles or UCAs, there exist many other systems, either natural or artificial, characterized by spherical (or more generally curved) geometries, with typical sizes ranging from micro to macro scale, which show evidences of complex spatio-temporal dynamics under external forcing [4]. Some problems of interest in this category are for example the vibrational modes of small liquid droplets or spherical molecules, or the buckling and rupture of UCAs.

We present here an experimental and numerical study of spatiotemporal dynamics in a parametrically driven system presenting a curved geometry. The system is a ring-shaped chain of coupled oscillators subjected to a vertical harmonic acceleration. The theoretical model is the well known Frenkel-Kontorova lattice (a discrete version of the sine-Gordon equation) with damping and parametric driving. A practical implementation of this chain (but in a straight configuration) was proposed in [5], where the existence of kinks was demonstrated. Later, the analysis was extended [6] to show the existence of breathers in this chain. Such a system, with the appropriate modifications, allows to investigate fundamental aspects not studied before, such as the effect of curvature in the existence and stability of the different localized solutions. Here we propose that a ring-type configuration of the linear 1D chain can be used as a toy model of acoustically driven UCA and related systems. We also investigate the effect of defects in the chain: nucleation of solitons, enhancement of stability. Thus, the aim of this work is twofold. On one hand, to study parametric instability leading to pattern formation and localized patterns (breathers and kinks) in a chain of coupled oscillators with circular symmetry (a ring) and, on the other hand, to show some formal analogies between this system and a spherical pulsating bubble. Our study could be useful to understand and predict localized solutions in bubbles, as certain localized modes observed experimentally [7], and to determine the optimal conditions for the excitation of particular patterns.

2 The Ring of Coupled Pendula

2.1 The Model

A driven-damped chain of coupled oscillators, despite its simplicity, is known to present a very rich dynamics, and is often used as a toy model to describe the behavior of other physical systems or processes, such as ladder networks of discrete Josephson junctions, charge-density wave-conductors, crystal dislocation in metals, DNA dynamics, and many others, see e.g. [8]. Most of these systems are well described by a straight chain. When disposed in the form of a circular ring, connecting first and last masses as we propose in this work, the chain forms the equivalent of a 2D bubble, and for small radius and/or large amplitudes the effect of curvature becomes non negligible. However, in the theoretical description below we will ignore for simplicity the curvature effects.

Let's consider a monoatomic pendulum lattice, formed by equal masses linearly coupled to their nearest neighbors. The whole chain is subjected to vertical oscillations (parametric driving) of amplitude A and angular frequency ω. The motion on the $n-th$ pendulum is described by its angle θ with respect to the vertical, which obeys the equation

$$\begin{aligned} & ml_n^2\ddot{\theta}_n + \gamma l_n\dot{\theta}_n + ml_n\left[g + 4A\omega^2\cos(2\omega t)\right]\sin(\theta_n) \\ & = k_2\left(\theta_{n+1} - 2\theta_n + \theta_{n-1}\right) + k_4\left[\left(\theta_{n+1} - \theta_n\right)^3 - \left(\theta_n - \theta_{n-1}\right)^3\right], \end{aligned} \tag{1}$$

where l_n is the length of the $n-th$ pendulum, m its mass, k_2 and k_4 are the nearest coupling strengths of the harmonic and quartic interactions respectively, γ is the friction coefficient and g the gravity constant acceleration. We note (see below) that the anharmonic coupling is included since it is related to the existence of upper cutoff breathers which are actually observed in the experiments. In this section, a homogeneous chain with identical elements is assumed, with $l_n = L$, but the effect of inhomogeneities will be considered later. After normalization, the homogeneous chain can be written in the form of a driven-damped Frenkel-Kontorova (FK) equation:

$$\begin{aligned} & \ddot{\theta}_n + \beta\dot{\theta}_n + \left[\omega_0^2 + \eta\cos(2\omega t)\right]\sin(\theta_n) \\ & = c_2\left(\theta_{n+1} - 2\theta_n + \theta_{n-1}\right) + c_4\left[\left(\theta_{n+1} - \theta_n\right)^3 - \left(\theta_n - \theta_{n-1}\right)^3\right] \end{aligned} \tag{2}$$

where $\eta = 4\omega^2 A/L$, $\omega_0 = \sqrt{g/L}$ is the natural frequency of the uncoupled system, $\beta = \gamma/ml$ and c_2, c_4 are the normalized damping and coupling terms, respectively. As stated, Eq. (2) does not take into account the curvature effect which are necessarily present in a ring geometry.

The type of localized solutions studied here (breathers and kinks) appear as a slow spatial modulation of the cutoff modes. In this case it is possible to derive equations describing the evolution of the envelopes. Following [5, 6] we consider solutions in the form

$$\theta_n(t) = \epsilon(\pm 1)^n \psi_\pm(\tau, x_n) \exp(-i\omega t) + c.c. \tag{3}$$

where ϵ is a smallness parameter and the positive (negative) sign describe modes existing close to the lower (upper) band edges, also called phase-matched and phase-mismatched modes respectively. Assuming the following scalings $\beta, \eta, (\omega^2 - \omega_\pm^2) \sim O(\epsilon^2)$, $\tau = \epsilon^2 t$, $x_n = \epsilon n a$, it follows that the amplitude of the envelope obeys the parametrically driven-damped nonlinear Schroedinger equation,

$$2i\omega_\pm \frac{\partial \psi_\pm}{\partial t} = c_2^2 \frac{\partial^2 \psi_\pm}{\partial x^2} + i\omega_\pm \beta \psi_\pm + \frac{\eta}{2}\psi_\pm^* + \chi_\pm \psi_\pm |\psi_\pm|^2 . \tag{4}$$

where $\omega_\pm = \{\omega_0, \sqrt{\omega_0^2 + 4c_2^2}\}$ and $\chi_\pm = \{\omega_0^2/2, \omega_0^2/2 - 96c_4^2\}$. Equation (4) has been derived for a variety of system in different disciplines (e.g. Faraday waves in vibrated fluid or granular layers, or pulses in optical fibers), differing only in the coefficients. Interestingly, it has been also derived in [11] to describe the azimuthal envelope of equatorial surface mode in bubbles. Thus, the ring of pendula is suitable for studying these solution which are characteristic of real bubbles. This and other analogies will be discussed also in Sect. 5.

2.2 Experimental Setup

The setup follows basically that proposed in [5], except for the circular geometry. The chain is formed by N spheres of mass m, suspended on a ring-shaped support of radius R by strings forming a "V" with vertical length L, Fig. 1. The coupling is obtained by overlapping the strings and fixing the crossing point with a knot at a distance d from the support. The whole system lies on a flat surface attached to a loudspeaker which provides the parametric driving. The images are taken with a camera located 1 m above the ring. For quantitative measurements of the amplitudes, optical correction was applied.

The linear (phonon) dispersion relation of the chain is bounded: it presents a lower cutoff frequency $\omega_l = \sqrt{g/L}$ and an upper cutoff frequency $\omega_u = \sqrt{g/(L-d)}$, which corresponds to the natural frequency of pendula oscillating either from the rigid support or from the knot, respectively. The dispersion relation can be obtained in the form

$$\left(\frac{\omega_n}{\omega_0}\right)^2 = \frac{1}{1-\eta}\left[1 - \eta \cos^2\left(\frac{\pi}{2}\frac{n}{N}\right)\right], \tag{5}$$

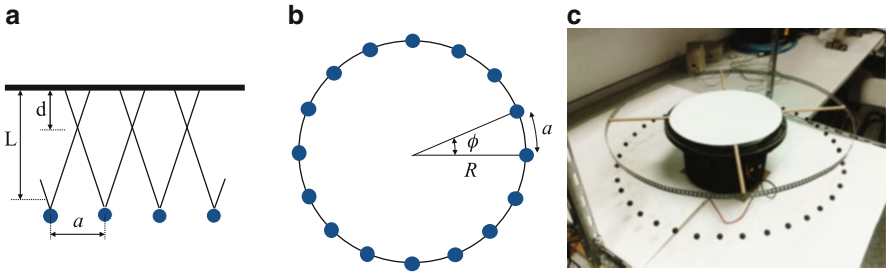


Fig. 1 Experimental setup: (**a**) side view (**b**) top view (**c**) photograph of the setup

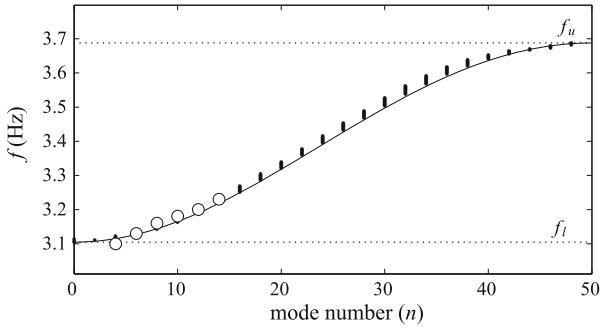


Fig. 2 Experimental eigenmodes (*open circles*) located on the theoretical dispersion curve. *Black circles* correspond to numerical results

where $\eta = d/L \in [0, 1]$ measures the strength of the coupling and n is the mode index number.

For the setup shown in Fig. 1 and used in our experiments, the parameters of the chain where $N = 39$ on the system shown on Fig. 1, $m = 5\,\text{g}$, $L = 10\,\text{cm}$, $d = 3\,\text{cm}$, $a = 5\,\text{cm}$, $R = 33\,\text{cm}$ (we note that the distances have a small variability along the chain, thus the experimental system is weakly inhomogeneous). For this set of parameters, the edges of the dispersion relation or cutoff frequencies, Eq. (5), occur at the frequencies $f = 3.11\,\text{Hz}$ and $f = 3.63\,\text{Hz}$ respectively (Fig. 2).

Because of the boundary conditions, in our closed system only even number of the mode index n are allowed. In Fig. 3 we show the first six eigenmodes excited in the system with increasing frequencies (see caption). The frequencies at which the different modes appear in the experiment follow the dispersion relation (5) with accuracy.

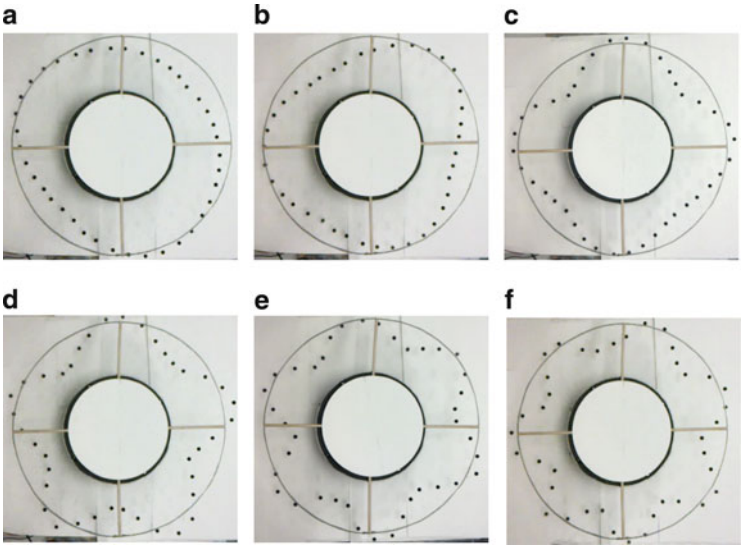


Fig. 3 Eigenmodes observed versus frequency of the parametric excitations: (**a**) 3.10 Hz, (**b**) 3.13 Hz, (**c**) 3.16 Hz, (**d**) 3.18 Hz, (**e**) 3.21 Hz, (**f**) 3.23 Hz

3 Localized Excitations

Driving the chain at frequencies slightly above or below the edges of the dispersion relation or phonon band, one can excite different types on localized modes in the chain. In this section we report the existence of four types of localized modes in the experimental ring chain described before. In a 1D linear (straight) chain, the motion of each oscillator is symmetric with respect to the angle [5]. For low amplitude oscillations, i.e. for linear modes, this is still a valid assumption for the ring-shaped chain. However, due to the curved geometry, this symmetry no more holds. The maximum amplitude is different in compression (motion towards the center of the ring) and expansion phases. Also the distance between neighbor oscillators shows such asymmetry, being larger for the expansion phase. This occurs because the masses approach or repel depending on the direction of motion. This effect is also observed in 3D (spherical) gas bubbles driven at large amplitude. In the following, we will ignore this effect. Note that the solutions given by Eq. (2) will not take into account this asymmetry, since curvature effects are not included there.

3.1 Lower Cutoff Modes

The NLS equation given by Eq. (4), predicts the existence of breathers at frequencies slightly below the lower cutoff. In Fig. 4, we show such localized solution, obtained

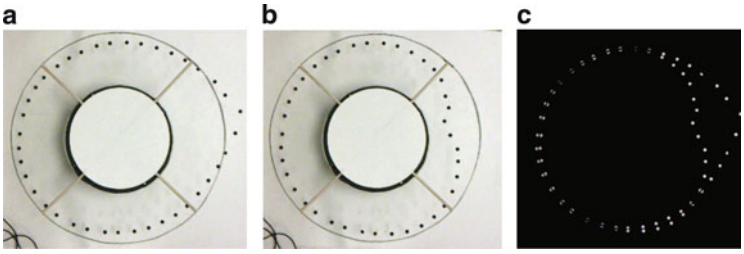


Fig. 4 Single breather as a example of localized solution (**a**): Maximum expansion phase; (**b**): Maximum compression phase; (**c**): Substraction between frames (**a**) and (**b**). Movie available at http://goo.gl/IK7RJ

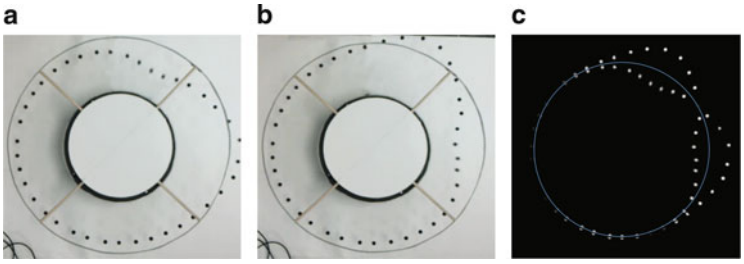


Fig. 5 A bound state of two breathers, at the same parameters as in Fig. 4. Movie available at http://goo.gl/nbPRP

by hitting a few oscillators when the chain is driven at $f = 3.03$ Hz. As in most of the paper, Fig. 4a, b show the chain distribution at the instant of maximum positive and negative peak amplitudes (expansion and compression phases, respectively), while figure (c) is the difference between both images, evidencing the breathing motion. Note the asymmetry between phases, as discussed above.

With the same parameters, one can easily excite also multiple-breather states. In Fig. 5 we show a bound state of two breathers, oscillating with opposite phases. Comparing with the single breather in Fig. 4, the bounded state presents distinctive features: the width of the individual breathers is smaller, their profiles (particularly in the compression phase) are smoothed, and the asymmetry in compression-expansion phases is enhanced.

We have also observed lower cutoff kinks, as those shown in Fig. 6. The kinks appear in pairs, and separate domains where a group of pendula oscillate with a given phase, shifted by π with respect to the neighbor domain. Differently from the nodes in the eigenmodes shown in Fig. 3, the distance between kinks (and the size of the domains) is arbitrary, and not fixed by the boundary conditions. We note that continuous theories based on NLS equations does not predict the existence of such lower cutoff kinks, even considering anharmonic coupling terms. This issue should be thus investigated further. Interestingly, kinks have still not been predicted to occur in gas bubbles.

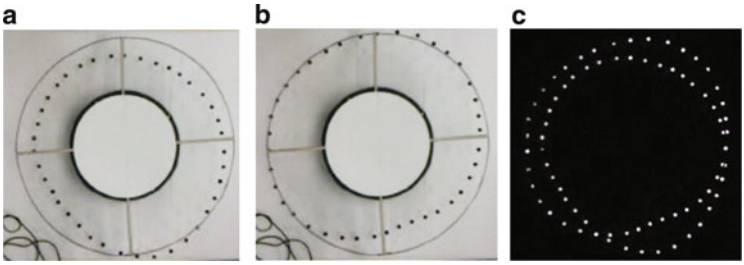


Fig. 6 Lower cutoff kink, obtained for a frequency $f = 3.08$ Hz

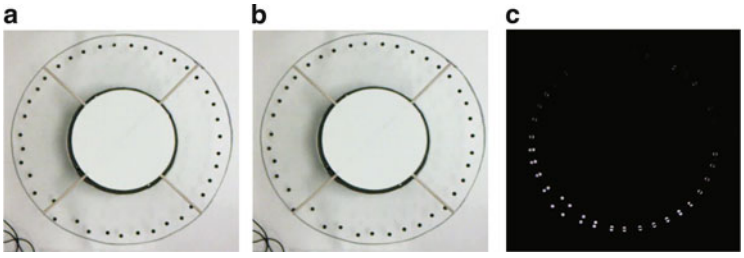


Fig. 7 Upper cutoff breather at $f = 4.0$ Hz. Movie available at http://goo.gl/h3Se5

These low frequency modes are more likely to be related to those observed in real gas bubbles, since oscillation of neighbor particles occurs in phase (as is always the case in a continuous system).

3.2 Upper Cutoff Modes

Both breathers and kinks exist for the chain at frequencies above the gap. This solutions do not find an equivalent in real bubbles (neighbor particles oscillate in anti-phase).

A remarkable fact is that the description of chain behavior as envelope wave solutions of the NLS equation [6] predicts that breather and kinks can not exist simultaneously in a given chain (they have incompatible existence domains). This is supported by the experimental observation in straight chains reported previously [9]. However, we have observed both structures (see figures) in our chain. This is another indication that the dynamics of our chain is not adequately described by continuous models of NLS type, and one must consider discreteness or curvature effects, which may enhance the stability domains. Also, the existence of weak randomness in the chain parameters may affect the stability of these structures. Both upper cutoff breathers and kinks are shown in Figs. 7 and 8 respectively.

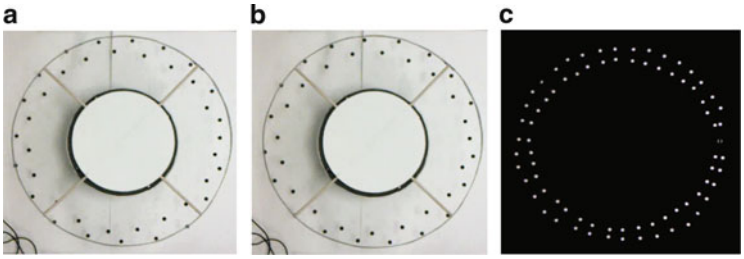


Fig. 8 Upper cutoff kink excited at $f = 4.1$ Hz. Movie available at http://goo.gl/hEOvy

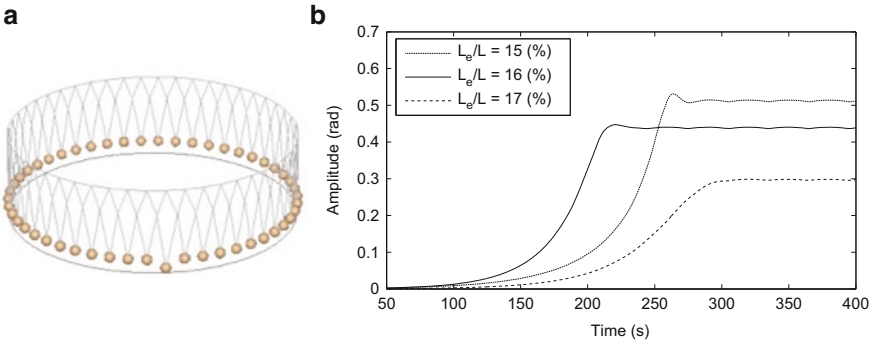


Fig. 9 (**a**) The ring chain with a point defect. (**b**) Time evolution of the breather amplitude, for different defect lengths

4 Defect-Induced Localization

The numerical study reveals that, in a perfectly homogeneous chain, localized solutions are difficult to excite, being very sensitive to the shape and amplitude of the initial condition. However, experimentally they appear much more easily, sometimes being enough to hit one oscillator to excite a breather or kink. Our experimental chain is far from ideal. There are no exactly equal oscillators, differing in the length, position of coupling knot, distance to the neighbors, etc. However it shows all the plethora of localized solutions described above, and predicted for the homogeneous chain. We have explored numerically the effect of two types of inhomogeneities in the chain: a localized defect (e.g. one pendulum with a length slightly different than the rest, Fig. 8a) and a random distribution of structural parameters. The effect of a single defect was discussed in [10], in the context of breather stabilization against space-time chaotic states. Applying a similar analysis to our ring chain, we observe and increase in the stabilization, according to our experimental observations. It occurs at particular values of the length of the defect: there exist an optimal length, at which the time of development of the breather is minimized, as shown in Fig. 8b). We also note that breathers tend to be localized at the defect position, a fact reported previously in the literature (Fig. 9).

5 Analogy with Gas Bubbles in an Ultrasound Field

The presented results about driven discrete chains in a ring configuration can be related to different observations reported for real gas bubbles driven by ultrasound fields, owing to the existing analogies between both systems. Here we review some basic results and subsequently highlight some of these analogies.

The literature on bubble dynamics is broad, since the problem has been investigated over the course of a century, starting from the seminal works of Rayleigh in 1912. Most of the efforts were devoted to describe the radial motion of a bubble under the action of an external pressure field, which is well described by the Rayleigh-Plesset equation for the time dependent radius $R(t)$

$$\rho\left(R\ddot{R}+\frac{3}{2}\dot{R}^2\right)=P_g-P_0-P_A(t)-\frac{2\sigma}{R}-4\mu\frac{\dot{R}}{R}, \tag{6}$$

with ρ the density of the surrounding fluid, $P_g = \left(P_0+\frac{2\sigma}{R_0}\right)\left(\frac{R_0}{R}\right)^{3\gamma}$, the gas pressure inside the bubble, P_0 is the hydrostatic pressure, R_0 is the equilibrium radius of the bubble, P_A the acoustic pressure, σ the surface tension of the bubble, μ the dynamic viscosity and γ the polytropic exponent.

Since acoustic vibrations are typically small in amplitude, one can often linearize the equations to get a simplified description. The radial vibration of a gas bubble in a fluid is well modeled as a simple harmonic oscillator whose stiffness and mass parameters relate to the properties of the gas and fluid. It is well known that the resonant frequency of the radial mode, known as the Minnaert frequency, is given by

$$f_0=\frac{1}{2\pi R_0}\sqrt{\frac{3\kappa p_0}{\rho_0}}. \tag{7}$$

For a microscopic bubble in water at standard pressure, this equation reduces to $f_0 R_0 = 3.26\,\mathrm{m/s}$. Note that a similar scaling relation roughly holds for our macroscopic bubble.

The analysis of surface modes in bubbles implies also the angular dependence, and becomes more complex. Two different theoretical approaches have been used. One consists in assuming that the radius can be expanded in terms of spherical harmonics, as

$$r(t,\theta,\phi)=R(t)+\sum_{n=0}^{i}a_i(t)Y_i(\theta,\phi). \tag{8}$$

When $|a_n| \ll R$ linearization leads to the following set of equations

$$\ddot{a}_n+\gamma_n\dot{a}_n+\omega_n^2 a_n=0 \tag{9}$$

where γ_n and ω_n are the damping and pulsation frequency of the different surface modes. In the stationary case $R(t) \to R_0$ they are given by

$$\begin{aligned} \gamma_n &= \frac{2(n+2)(2n+1)\mu}{\rho R^2} \\ \omega_n^2 &= \frac{(n-1)(n+1)(n+2)\sigma}{\rho R^3} \end{aligned} \tag{10}$$

Similar equations can be obtained, with different coefficients, for the macroscopic ring of pendula.

A different approach, which does not require linearization, has been followed in [11]. Starting from the Hamiltonian of the fluid system and using a multiple-scales expansion, an amplitude equation for the envelopes was derived.

Consider a solution in the form

$$r(t,\theta,\phi) = R_0 + \left(\frac{1}{2}\rho(\theta,t)e^{-i\omega t} + c.c.\right)\cos(n\phi) \tag{11}$$

then, it is shown that the amplitude obeys the equation

$$2i\omega\frac{\partial\rho}{\partial t} = \Delta\rho + c^2\frac{\partial^2\rho}{\partial x^2} + 2i\omega\delta\rho + \beta\rho^* + \alpha\rho\left|\rho\right|^2. \tag{12}$$

where $x = \cos(\theta)$ and

$$\begin{aligned} \Delta &= (\omega_1^2 - \omega^2) + \omega_1^2\left(\tfrac{5}{8n} + \tfrac{3x^2}{2}\right) \\ c^2 &= \tfrac{3\omega_1^2}{2n^2} \\ \alpha &= \tfrac{17}{32}\omega_1^2\left(\tfrac{n}{R_0}\right)^2 \end{aligned} \tag{13}$$

where $\omega_1^2 = (n-1)(n+1)(n+2)\sigma/(\rho R_0^3)$ and β and δ are parametric driving and losses introduced phenomenologically. This equation is structurally similar to the equation obtained for the chain of pendula, Eq. (4), but with different coefficients. The study predicts the existence of localized patterns on the bubble wall, as shown in[11], similar to those reported here for the macroscopic bubble pendula.

6 Conclusions

The spatio-temporal dynamics of a parametrically driven array of coupled oscillators forming a closed line or ring has been investigated. We demonstrate experimentally the existence of four types of localized solutions, in the form of kinks and breathers. These structures show particular features related to the asymmetry introduced by the curvature of the system. The effect of inhomogeneities in the chain is also discussed. This macroscopic system shows similarities with the acoustically

driven gas bubble, where the parametric driving is exerted by a harmonic ultrasound field. We compared here both systems to show possible relations between the localized patterns that can be used novel features in gas bubble dynamics (e.g., the existence of kinks). However, formal techniques as the Similarity Analysis (SA) can be used to explore quantitatively the limits of this analogies. Work in this direction is in progress.

Acknowledgements The work was supported by Spanish Ministry of Science and Innovation and European Union FEDER through project FIS2011-29731-C02-02.

References

1. T. Leighton , *The Acoustic Bubble* (Academic, London, 1997)
2. A.I. Eller, L.A. Crum, Instability of the motion of a pulsating bubble in a sound field. J. Acoust. Soc. Am. **47**, 762 (1970)
3. A. Prosperetti, Viscous effects on perturbed spherical flows. Appl. Math. **84**, 339 (1977)
4. A.O. Maksimov, T. Leighton, Pattern formation on the surface of a bubble driven by an acoustic field. Proc. R. Soc. A **468**, 57 (2011)
5. B. Denardo, B. Galvin, A. Greenfield, A. Larraza, S. Putterman, W. Wright, Observations of localized structures in nonlinear lattices: domain walls and kinks. Phys. Rev. Lett. **68**, 1730 (1992)
6. W.-Z. Chen, Experimental observation of solitons in a 1D nonlinear lattice. Phys. Rev. B. **49**, 15063 (1994)
7. M. Versluis, D.E. Goertz, P. Palanchon, I.L. Heitman, S.M. van der Meer, B. Dollet, N. de Jong, D. Lohse, Microbubble shape oscillations excited through ultrasonic parametric driving. Phys. Rev. E **82** (2010)
8. O.M. Braun, Y.S. Kivshar, *The Frenkel-Kontorova model: Concepts, Methods and Applications* (Springer, Berlin/New York, 2004)
9. J. Cuevas, L.Q. English, P.G. Kevrekidis, M. Anderson, Discrete breathers in a forced-damped array of coupled pendula: modeling, computation, and experiment. Phys. Rev. Lett. 102, 224101 (2009)
10. N.V. Alexeeva, I.V. Barashenkov, G.P. Tsironis, Impurity-induced stabilization of solitons in arrays of parametrically driven nonlinear oscillators. Phys. Rev. Lett. **84**, 3053 (2000)
11. A.O. Maksimov, T.G. Leighton, P.R. Birkin, Self focusing of acoustically excited Faraday ripples on a bubble wall. Phys. Lett. A **372**, 3210 (2008)